Quantum degenerate Majorana surface zero modes in two-dimensional space

Ching-Yu Huang,[1] Yen-Ting Lin,[2] Hao Lee,[3,4] and Daw-Wei Wang[1,3,5]
[1]*Physics Division, National Center for Theoretical Sciences, Hsinchu, Taiwan*
[2]*Institute for Theory of Statistical Physics, RWTH Aachen, 52056 Aachen, Germany*
[3]*Physics Department, National Tsing Hua University, Hsinchu, Taiwan*
[4]*Imagination Broadway Ltd., New Taipei City, Taiwan*
[5]*Center for Quantum Technology and Department of Physics, National Tsing Hua University, Hsinchu 30013, Taiwan*

(Received 27 July 2017; published 24 April 2019)

We investigate the topological properties of spin-polarized fermionic polar molecules loaded in a multilayer structure with the electric dipole moment polarized to the normal direction. When polar molecules are paired by attractive interlayer interaction, unpaired Majorana fermions can be macroscopically generated in the top and bottom layers in dilute density regime. We show that the resulting topological state is effectively composed by a bundle of one-dimensional (1D) Kitaev ladders labeled by in-plane momenta $\mathbf{k}_\parallel$ and $-\mathbf{k}_\parallel$, and hence belongs to the *BDI* class characterized by the winding number $\mathbb{Z}$, protected by the time-reversal symmetry. The Majorana surface modes exhibit a flat band at zero energy, fully gapped from Bogoliubov excitations in the bulk, and hence becomes an ideal system to investigate the interaction effects on quantum degenerate Majorana fermions. We further show that additional interference fringes can be identified as a signature of such 2D Majorana surface modes in the time-of-flight experiment.

DOI: 10.1103/PhysRevA.99.043624

I. INTRODUCTION

A Majorana fermion (MF) is known to be its own antiparticle [1], as a hypothesis in theoretical particle physics. In condensed-matter systems, a MF can appear as a localized edge state and reflect the topological property in the bulk of system. It is known that a topological system can be classified into intrinsic topological order or symmetry-protected topological (SPT) order: the latter is robust against small perturbations for given on-site symmetries [2]. Ground states of nontrivial SPT phases cannot be continuously connected to trivial product states without either closing the gap or breaking the protecting symmetry [3].

One of the mostly studied topological phases is proposed by Kitaev [4] for a one-dimensional (1D) *p*-wave superconductor. The Majorana zero mode (MZM) of such a system may be applied for quantum computation through braiding, and a certain experimental signature has been proposed in an ordinary *s*-wave superconducting wire with strong spin-orbital coupling through the proximity effect [5–14] or even in systems of ultracold atoms [15–19]. However nonambiguous evidence is still lacking probably due to the poor signal-to-noise ratio for a localized MZM. Recently, some extensions of the 1D Kitaev model by including interchain tunneling [20], dimerization [21], and long-ranged pairing [22,23] have also been proposed.

In the systems of quantum gases, such intersite pairing between fermions can be provided by long-ranged dipolar interactions between polar molecules [24–29] or neutral atoms with a large magnetic moment [30–32]. Since the inelastic coupling between polar molecules can be well suppressed by aligning dipole moments normal to the two-dimensional (2D) plane with a strong transverse confinement [33–35], many exotic ground states have been predicted in a 2D layer [36–49] or in a bilayer or multilayer structure [39,44,46,50–52].

In this paper, we propose that macroscopically degenerate Majorana surface zero modes (MSZMs) can exist in a 2D continuous space, where spin-polarized fermionic polar molecules are paired and hence perform a superfluid in a stack of multilayer structure [Fig. 1(a)] through their dipolar interaction. Within the BCS theory and Landau-Fermi-liquid theory (both are well justified in our 3D system), we show that the multilayer system becomes equivalent to an ensemble of 1D Kitaev ladders along the normal direction [see Fig. 1(b)], labeled by in-plane momenta ($\mathbf{k}_\parallel$, $-\mathbf{k}_\parallel$). That is, each subsector is equivalent to the BdG Hamiltonian of 1D Kitaev ladders. The resulting topological state actually belongs to the *BDI* class, characterized by the $\mathbb{Z}$ index as the winding number. The associated topological properties are confirmed by both the analytical calculation as well as the numerical calculation of entanglement spectrum or entropy when the long-range pairing is included. These unpaired MSZMs are protected by the time-reversal symmetry as well as the superfluid pairing gap, showing a localized wave function along the normal direction of layers (z) and a mobile flat energy band in the in-plane direction (x-y) inside the superfluid gap. From an experimental point of view, such a topological state can be observed through the additional short period interference fringes, which result from macroscopically occupied MSZMs in the top and bottom layers. Our results therefore suggest an interesting system to investigate quantum many-body properties of non-Abelian anyons in a 2D continuous space.

Our paper is organized as follows: in Sec. II, we set up a system which is loaded into a stack of 2D layers with spin-polarized fermionic polar molecules, and derive the effective model Hamiltonian within the mean-field approximation.

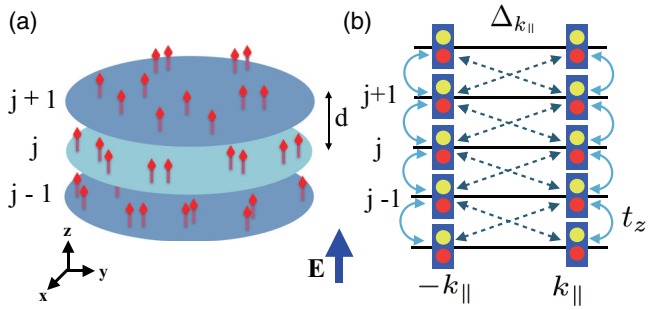

FIG. 1. (a) Multilayer structure for identical fermionic polar molecules loaded into a deep 1D optical lattice. The electric dipole moment (arrows) is aligned to the normal (z) direction by the external field. (b) Effective Kitaev ladder in momentum space [see Eq. (2)], where fermions (rectangular boxes) in each "site" can be decomposed into two MFs (circles, see the text). Two unpaired MFs can be found at the end of ladders if Eq. (10) is satisfied. Double-sided arrows of dashed (solid) lines indicate interlayer pairing (hopping) respectively (for simplicity, here we just show the configuration of a special case, where only pairs between neighboring layers are considered; see Sec. III A).

In Sec. III, we investigate the topological properties and Majorana surface zero modes of a special case, where only the nearest pairing is considered. We then extend our calculation in Sec. IV toward a more general case when the long-ranged pairing (due to dipolar interaction) is included. In Sec. V we show why these MFs are stable against single-particle perturbation due to the time-reversal symmetry. Finally we discuss some experimentally related issues in Sec. VI and conclude our paper in Sec. VII. In Appendix A, we show how the unpaired MFs can be analytically obtained from the Bogoliubov–de Gennes (BdG) equation. We then explicitly calculate the winding number in Appendix B.

II. SYSTEM HAMILTONIAN

A. Full Hamiltonian and mean-field approximations

The system setup is illustrated in Fig. 1(a), where spin-polarized fermionic polar molecules are loaded into a stack of 2D layers with interlayer spacing d and tunneling amplitude t_z. The electric dipole moment is polarized and perpendicular to the layer by the external electric field, leading to an attractive interlayer interaction and a repulsive intralayer interaction between molecules. As a result, the full system Hamiltonian can be expressed as follows in the real-space coordinates:

$$\begin{aligned} H = & -t_z \sum_{j=1}^{L-1} \int d\mathbf{r}_\parallel [\psi_j(\mathbf{r}_\parallel)^\dagger \psi_{j+1}(\mathbf{r}_\parallel) + \text{H.c.}] \\ & + \sum_{j=1}^{L} \int d\mathbf{r}_\parallel \psi_j(\mathbf{r})^\dagger \left[\frac{-\nabla^2}{2m} + U_{\text{trap}}(\mathbf{r}_\parallel) - \mu \right] \psi_j(\mathbf{r}_\parallel) \\ & + \frac{1}{2} \sum_{j,j'=1}^{L} \int d\mathbf{r}_\parallel \int d\mathbf{r}'_\parallel V_d(\mathbf{r}_\parallel - \mathbf{r}'_\parallel, jd - j'd) \psi_j(\mathbf{r}_\parallel)^\dagger \\ & \times \psi_{j'}(\mathbf{r}'_\parallel)^\dagger \psi_{j'}(\mathbf{r}'_\parallel) \psi_j(\mathbf{r}_\parallel), \end{aligned} \tag{1}$$

where m and μ are the mass and chemical potential of polar molecules. $\psi_j(\mathbf{r}_\parallel)$ is the field operator for the layer index j and the in-plane coordinate $\mathbf{r}_\parallel$. $V_d(\mathbf{r}_\parallel, z)$ is the dipole-dipole interaction between polar molecules. Here for simplicity, we assume the layer width is much smaller than interlayer distance and can be neglected. $U_{\text{trap}}(\mathbf{r}_\parallel)$ is the in-plane trapping potential, and $L \gg 1$ is the number of total layers.

Since the multilayer structure described above is actually a quasi-3D system, ordinary mean-field approximations are well justified. In order to highlight the possibility of SPT order in such 3D systems, we consider the parameter regime when the averaged in-plane density is in the dilute regime, i.e., the averaged interparticle distance between molecules in the same layer is larger than the interlayer distance. It is then reasonable to expect that the effects of in-plane repulsive interaction ($\sim |\mathbf{r}_\parallel|^{-3}$) are relatively weaker than both the in-plane kinetic energy and the effects of interlayer attractive interaction (see Sec. VI below for more details). As a result, the attractive interlayer interaction pairs up polar molecules in different layers as a superfluid phase within the BCS theory. By contrast, the repulsive interaction between molecules in the same layer is a relatively weak effect, renormalizing the effective mass and chemical potential within the Landau-Fermi-liquid theory [39,53]. Throughout this paper, we will *not* discuss the situation when the in-plane repulsion becomes relevant, which appears only in the high-density regime. We will briefly discuss its possible effects in Sec. V.

B. Effective Hamiltonian of Kitaev ladders

In the rest of this paper, we consider that the trapping potential $U_{\text{trap}}(\mathbf{r}_\parallel)$ is assumed to be shallow enough so that we could neglect it and apply a periodic boundary condition in the in-plane (x-y) direction. We will discuss the situation of the finite-size effect in Sec. V and show it should be instant to the stability of the topological properties. As a result, within the mean-field approximations mentioned above, an effective Bogoliubov–de Gennes (BdG) Hamiltonian can be easily derived to be $H_{\text{BdG}} = \sum_{\mathbf{k}_\parallel} H_{\mathbf{k}_\parallel}$, where

$$\begin{aligned} H_{\mathbf{k}_\parallel} = & \sum_{j=1}^{L} \left(\frac{\mathbf{k}_\parallel^2}{2m^*} - \mu^* \right) c^\dagger_{\mathbf{k}_\parallel, j} c_{\mathbf{k}_\parallel, j} \\ & - t_z^* \sum_{j=1}^{L-1} [c^\dagger_{\mathbf{k}_\parallel, j} c_{\mathbf{k}_\parallel, j+1} + \text{H.c.}] \\ & - \frac{1}{2} \sum_{j \neq j', jj'=1}^{L} \Delta_{\mathbf{k}_\parallel}^{(|j'-j|)} [c^\dagger_{\mathbf{k}_\parallel, j} c^\dagger_{-\mathbf{k}_\parallel, j'} + \text{H.c.}]. \end{aligned} \tag{2}$$

Here $c_{\mathbf{k}_\parallel, j} = \frac{1}{\sqrt{\Omega}} \int d\mathbf{r}_\parallel \psi_j(\mathbf{r}_\parallel) e^{-i\mathbf{k}_\parallel \cdot \mathbf{r}_\parallel}$ is the field operator of the jth layer and the in-plane momentum $\mathbf{k}_\parallel$. Ω is the area of the 2D layer; μ^*, m^*, and t_z^* are the renormalized chemical potential, molecule mass, and interlayer tunneling amplitude respectively. $\Delta_{\mathbf{k}_\parallel}^{(|j'-j|)}$ is the gap function between the jth and j'th layers by defining $\Delta_{\mathbf{k}_\parallel}^{(|j'-j|)} = -\sum_{\mathbf{k}'_\parallel} V_d(\mathbf{k}_\parallel, \mathbf{k}'_\parallel, j, j') \langle c_{\mathbf{k}_\parallel, j} c_{-\mathbf{k}_\parallel, j'} \rangle$. Here we make a Fourier transform of dipole-dipole interaction $V_d(\mathbf{r}_\parallel, z)$ into momentum space, and we find that (see Ref. [44]) $V_d(\mathbf{k}_\parallel, \mathbf{k}'_\parallel, j, j') \rightarrow$

$-2\pi|\mathbf{k}_\parallel|e^{-|\mathbf{k}_\parallel|d}$ as $W/d \to 0$ (W and d are the layer width and interlayer spacing). Therefore, the interlayer dipolar interaction is attractive for the whole momentum transfer in momentum space.

One can see that, if we define

$$H^{\text{ladd}}_{\mathbf{k}_\parallel} \equiv H_{\mathbf{k}_\parallel} + H_{-\mathbf{k}_\parallel}, \tag{3}$$

$H^{\text{ladd}}_{\mathbf{k}_\parallel}$ is nothing but a two-leg Kitaev ladder in *momentum space*, where the topological properties (if they exist) are obviously protected by time-reversal, particle-hole, and chiral symmetries at the same time, and hence belongs to the *BDI* class of Altland-Zirnbauer classification [2]. Here the time-reversal symmetry is effectively protected, because polar molecules can be initially prepared in the same hyperfine state with a polarized spin state [54]. And, their exchange interaction is known to be so weak that spin relaxation is almost frozen during the experimental holding time.

III. MSZMs FOR THE NEAREST-NEIGHBOR PAIRING

In order to investigate the possible topological properties of the Kitaev ladder in momentum space, we would start from a specific model, where superfluid pairing appears only between nearest-neighboring layers, i.e., $\Delta^{(|j'-j|)}_{\mathbf{k}_\parallel} = 0$ for $|j-j'| \geqslant 2$. Results including longer range interaction will be discussed in the next section.

A. Exact solution of a special case

First, we show the exact solution of a special case and then calculate the winding number for a general situation. We consider a special situation when $\mathbf{k}^2_\parallel/2m^* - \mu^* = 0$ and $\Delta_{\mathbf{k}_\parallel} \equiv \Delta^{(1)}_{\mathbf{k}_\parallel} = t^*_z$. This special choice makes the ladder Hamiltonian $H^{\text{ladd}}_{\mathbf{k}_\parallel}$ have a single energy scale only.

We then define MFs in momentum space to be

$$\gamma^{(1)}_{\mathbf{k}_\parallel,j} \equiv c_{\mathbf{k}_\parallel,j} + c^\dagger_{-\mathbf{k}_\parallel,j} \quad \gamma^{(2)}_{\mathbf{k}_\parallel,j} \equiv -i(c_{\mathbf{k}_\parallel,j} - c^\dagger_{-\mathbf{k}_\parallel,j}), \tag{4}$$

with the anticommutation relations $\{\gamma^{(a)}_{\mathbf{k}_\parallel,j}, \gamma^{(b)}_{\mathbf{k}'_\parallel,j'}\} = 2\delta_{j,j'}\delta_{a,b}\delta_{\mathbf{k}_\parallel,-\mathbf{k}'_\parallel}$ ($a,b = 1,2$). After some algebra, we obtain (see Appendix A)

$$H^{\text{ladd}}_{\mathbf{k}_\parallel} = it^*_z \sum_{j=1}^{L-1} \left(\gamma^{(2)}_{\mathbf{k}_\parallel,j}\gamma^{(1)}_{-\mathbf{k}_\parallel,j+1} + \gamma^{(2)}_{-\mathbf{k}_\parallel,j}\gamma^{(1)}_{\mathbf{k}_\parallel,j+1}\right), \tag{5}$$

where the ladder Hamiltonian becomes two decoupled chains with two MFs missed at each end [see Fig. 1(b)]: $\gamma^{(1)}_{\pm\mathbf{k}_\parallel,1}$ for the bottom layer ($j = 1$), and $\gamma^{(2)}_{\pm\mathbf{k}_\parallel,L}$ for the top layer ($j = L$). One can easily construct two "real" MFs in each layer by defining $\bar{\gamma}^{(a)}_{\pm,\mathbf{k}_\parallel} = (\pm 1)^{1/2}(\gamma^{(a)}_{\mathbf{k}_\parallel} \pm \gamma^{(a)}_{-\mathbf{k}_\parallel})$, which is its own antiparticle: $(\bar{\gamma}^{(a)}_{\pm,\mathbf{k}_\parallel})^\dagger = \bar{\gamma}^{(a)}_{\pm,\mathbf{k}_\parallel}$ $a = 1,2$.

It is easy to show that, even for ladders with $k^2_\parallel/2m \neq \mu$ or $\Delta_{\mathbf{k}_\parallel} \neq t^*_z$, we could still diagonalize $H^{\text{ladd}}_{\mathbf{k}_\parallel}$ by introducing new MFs, $\tilde{\gamma}^{(a)}_{\mathbf{k}_\parallel,l}$, which is a linear combination of $\gamma^{(a)}_{\mathbf{k}_\parallel,j}$ ($a = 1,2$), and satisfies $\{\tilde{\gamma}^{(a)}_{\mathbf{k}_\parallel,l}, \tilde{\gamma}^{(b)}_{\mathbf{k}'_\parallel,l'}\} = 2\delta_{l,l'}\delta_{a,b}\delta_{\mathbf{k}_\parallel,-\mathbf{k}'_\parallel}$. Localized MFs, $\tilde{\gamma}^{(1)}_{\pm\mathbf{k}_\parallel,j=1/L}$, near the bottom or top layer can be still retained when some condition is satisfied (see below). It is just an extension of the 1D Kitaev chain to the two-ladder case in momentum space.

B. General condition for MSZMs

The topological property of our Kitaev ladder in momentum space can be further investigated by calculating the winding number with a periodic boundary condition along the normal (z) direction. After applying Fourier transform on the Hamiltonian [Eq. (2)] along the z direction. For simplicity, here we just consider the nearest-neighboring pairing only, although it can be in principle applied to a more general situation. Defining the Nambu spinor, $C_{k_\parallel,k_z} = [c_{k_\parallel,k_z}, c^\dagger_{-k_\parallel,-k_z}]^T$, we obtain

$$H_{\text{BdG}} = \frac{1}{2}\sum_{k_\parallel}\sum_{k_z} C^\dagger_{k_\parallel,k_z}\begin{bmatrix}\xi_{\mathbf{k}} & \tilde{\Delta}^\dagger_{\mathbf{k}} \\ \tilde{\Delta}_{\mathbf{k}} & -\xi_{\mathbf{k}}\end{bmatrix}C_{k_\parallel,k_z}, \tag{6}$$

where $\xi_{\mathbf{k}} \equiv \mathbf{k}^2_\parallel/2m^* - \mu^* - 2t^*_z\cos(k_z d)$. Note that we define the 3D momentum $\mathbf{k} \equiv (\mathbf{k}_\parallel, k_z)$ and the 3D gap function $\tilde{\Delta}_{\mathbf{k}} \equiv 2i\Delta_{\mathbf{k}_\parallel}\sin(k_z d)$ for the convenience of later discussion. The Bogoliubov excitation energies are given by

$$\begin{aligned} E^{(\pm)}_{\mathbf{k}} &= \pm\sqrt{\xi^2_{\mathbf{k}} + |\tilde{\Delta}_{\mathbf{k}}|^2} \\ &= \pm\sqrt{\xi^2_{\mathbf{k}} + 4|\Delta_{\mathbf{k}_\parallel}|^2\sin^2(k_z d)}. \end{aligned} \tag{7}$$

The gap is closed at $k_z = 0$ or π/d, and $\xi_{\mathbf{k}} \equiv \mathbf{k}^2_\parallel/2m^* - \mu^* - 2t^*_z\cos(k_z d) = \mathbf{k}^2_\parallel/2m^* \mp \mu^* - 2t^*_z = 0$.

To calculate the winding number of the Bloch state wave function, we first apply a unitary transformation on the BdG Hamiltonian to make it off-diagonal,

$$H_{\text{BdG}} = \frac{i}{4}\sum_{\mathbf{k}} \Gamma^\dagger_{\mathbf{k}}\begin{bmatrix}0 & v_{\mathbf{k}} \\ v^\dagger_{\mathbf{k}} & 0\end{bmatrix}\Gamma_{\mathbf{k}}, \tag{8}$$

with $v_{\mathbf{k}} \equiv \xi_{\mathbf{k}} + \frac{1}{2}(\tilde{\Delta}^*_{\mathbf{k}} - \tilde{\Delta}_{\mathbf{k}}) = \xi_{\mathbf{k}} - 2i\Delta_{\mathbf{k}_\parallel}\sin(k_z d) \equiv R(\mathbf{k})e^{i\theta(\mathbf{k})}$ and $\Gamma_{\mathbf{k}} \equiv [c_{\mathbf{k}} + c^\dagger_{-\mathbf{k}}, -ic_{\mathbf{k}} + ic^\dagger_{-\mathbf{k}}]^T$.

The winding number can be calculated as follows (see Appendix B for details):

$$\begin{aligned} W_{\mathbf{k}_\parallel} &\equiv \int_{-\pi/d}^{\pi/d}\frac{dk_z}{2\pi}\partial_{k_z}\theta_{\mathbf{k}_\parallel,k_z} \\ &= \frac{J_-}{2}\oint\frac{dz}{2\pi i}\frac{z^2 + 2J_+ z + 1}{J_1 J_2\prod_{j=1}^4(z - Z_j)}, \end{aligned} \tag{9}$$

where $\mu^*_{\mathbf{k}_\parallel} \equiv \mu^* - \mathbf{k}^2_\parallel/2m^*$, $J_1 = \frac{t^*_z + \Delta_{\mathbf{k}_\parallel}}{\mu^*_{\mathbf{k}_\parallel}}$, $J_2 = \frac{t^*_z - \Delta_{\mathbf{k}_\parallel}}{\mu^*_{\mathbf{k}_\parallel}}$, and $J_\pm = J_1 \pm J_2$. Four poles of the integrand are given as $Z_{1,2} = \frac{-1\pm\sqrt{1-4J_1J_2}}{2J_1}$ and $Z_{3,4} = \frac{-1\pm\sqrt{1-4J_1J_2}}{2J_2}$ respectively. One can find that $W_{\mathbf{k}_\parallel}$ become nonzero (i.e., topological nontrivial) only when the following condition is satisfied:

$$\left|\mu^* - \frac{\mathbf{k}^2_\parallel}{2m^*}\right| < 2t^*_z, \tag{10}$$

which is independent of the gap function as expected. This condition fails as $\mathbf{k}^2_\parallel/2m^* \pm 2t_z = \mu^*$, exactly when the Bogoliubov excitation energy becomes gapless at $k_z = 0$ and π/d [see Eq. (7)].

From Eq. (10), the Majorana surface modes appears when the in-plane momentum is within a certain range:

$$k_{\mathrm{Min}} < |\mathbf{k}_\parallel| < k_{\mathrm{Max}}, \tag{11}$$

where $k_{\mathrm{Min}} \equiv \sqrt{2m^*[\mathrm{Max}(0, \mu^* - 2t_z^*)]}$ and $k_{\mathrm{Max}} \equiv \sqrt{2m^*(\mu^* + 2t_z^*)}$ respectively.

Throughout this paper, we will consider the situation when $t_z^* > \mu^*/2$ *only*, so that $k_{\mathrm{Min}} = 0$ and ladders of *all* in-plane momenta for $|\mathbf{k}_\parallel| < k_{\mathrm{Max}}$ are topologically nontrivial. (Note that k_{Max} is also the largest Fermi momentum around the Fermi sea at $k_z = 0$.) Under this condition, the Majorana modes occupy the whole in-plane Fermi sea in the top and bottom layers. From the energy point of view, these unpaired MFs stay in the middle of the superfluid gap. As for the situation when $\mu^* > 2t_z^*$, only those states with in-plane momenta, $k_{\mathrm{Min}} < |\mathbf{k}_\parallel| < k_{\mathrm{Max}}$, are possible states with topological nontrivial properties. However, as we will show later, the topological properties of such a case may become unstable against disorder potential. We will therefore not emphasize this case in the rest of this paper.

IV. MSZMs FOR A LONG-RANGED PARING

In this section, we will include the long-ranged pairing order parameter into the Kitaev ladder [see Eqs. (2) and (3)], where the pairing amplitude is expected to be $\Delta_{\mathbf{k}_\parallel}^{(|j-j'|)} = \Delta_{\mathbf{k}_\parallel}^{(1)} \times |j - j'|^{-3}$, due to the dipolar interaction. The major goal is to investigate if the longer-ranged pairing will make such a topological state unstable or to change the boundary of the phase diagram, compared to the nearest-neighboring pairing in the last section. In principle, we could repeat the calculation of the winding number and investigate the effects of longer-range pairing. However, the analytical calculation becomes much more complicated and hence less intuitive.

Therefore, we will show numerical results based on the entanglement spectrum and entropy as well as the exact diagonalization methods. Both of them confirm the topological properties even with dipolar interaction.

A. Full numerical calculation of entanglement spectrum and entanglement entropy

A topological phase can be also characterized by the quantum entanglement between the subsystem and the environment [55–59]. In short, given a ground-state wave function $|\Psi\rangle$, one can calculate the reduced density matrix ρ_A for a subsystem A by tracing over the environment [see Fig. 2(a)]. The eigenvalue λ_α of the reduced density matrix is the so-called "entanglement spectrum" [57], which carries nonlocal information and has been applied for calculating Berry phase and zero-energy edge states [60]. For example, the degeneracy of the entanglement spectrum has recently been implemented to characterize the topological properties for some 2D quantum Hall states [57] and for some 1D SPT phases [58,59].

For the 1D Kitaev model, λ_α is given by the eigenvalues of the block's Green's-function matrix, i.e., $G_{\mathbf{k}_\parallel,i,j} \equiv \langle c_{\mathbf{k}_\parallel,i} c_{\mathbf{k}_\parallel,j}^\dagger \rangle$ with the layer indices i and j inside the subsystem A. In Refs. [60–62], it has been shown that the zero energy mode of the 1D Kitaev model corresponds to the degeneracy of $\lambda_\alpha = 1/2$ in the entanglement spectrum, i.e., the pair of zero modes at two ends of Kitaev chain contribute the maximal entanglement between subsystem A and the environment. Besides the entanglement spectrum, a topological phase transition can be also identified by the discontinuity of the entanglement entropy of the subsystem (given by $S_A = -\mathrm{Tr}[\rho_A \ln \rho_A]$) after tracing out the environment.

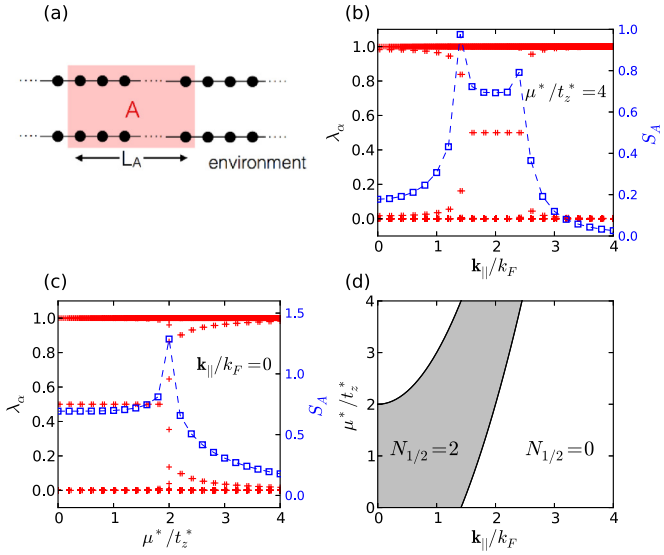

FIG. 2. (a) The whole system is divided into finite subsystem A with L_A sites and environment. Here we consider $L \gg L_A \gg 1$. Panel (b) shows the entanglement spectrum λ_α (red plus), and the entanglement entropy S_A (blue square) as a function of $\mathbf{k}_\parallel/k_F$ for $\mu^* = 4t_z^*$. Here $k_F \equiv \sqrt{2m^*\mu^*}$. Panel (c) is the same as (b) but as a function of μ^*/t_z^* for $\mathbf{k}_\parallel = 0$. (d) Phase diagram of the topological regime calculated from entanglement spectrum. $N_{1/2}$ is the number of the degeneracy in the entanglement spectrum at $\lambda_\alpha = 1/2$ for the subsystem A. This also indicates the number of MFs at the edge. The upper and lower boundaries are exactly the same as k_{Min} and k_{Max} calculated from Eq. (10).

It has been shown that the entanglement spectrum λ_α of subsystem A can be obtained by diagonalizing the entire Green's-function matrix $G_{\mathbf{k}_\parallel,m,n}$ [60–62], where m and n are restricted in subsystem A (along the z direction) with wave number $\mathbf{k}_\parallel$.

To calculate the Green's function, we first express the full mean-field Hamiltonian in another form [see Eq. (6)]: $H_{\mathrm{BdG}} = \frac{1}{2}\sum_{\mathbf{k}_\parallel,k_z} C_{\mathbf{k}_\parallel,k_z}^\dagger [\mathbf{R}(\mathbf{k}) \cdot \vec{\sigma}] C_{\mathbf{k}_\parallel,k_z}$, where $\vec{\sigma} = (\sigma_x, \sigma_y, \sigma_z)$ are Pauli matrices and $R(\mathbf{k}) \equiv (0, \tilde{\Delta}_\mathbf{k}, \xi_\mathbf{k})$. As a result, the Green's-function matrix defined in real-space lattice sites (i.e., layer),

$$G_{\mathbf{k}_\parallel,m,n} = \frac{1}{L}\sum_{k_z \in BZ} e^{ik_z(m-n)d} G_\mathbf{k}, \tag{12}$$

where d is the interlayer distance, L is the total number sites of the z direction, and k_z takes values in the first Brillouin zone. It is worth mentioning that $G_\mathbf{k}$ is a 2×2 matrix, $G_\mathbf{k} = \frac{1}{2}(1 + \frac{\mathbf{R}(\mathbf{k})\cdot\vec{\sigma}}{|\mathbf{R}(\mathbf{k})|})$.

In our case, we numerically diagonalize the block's Green's function for subsystem A with a finite size, e.g., $L_A = 100$ and $L = 200$, of the ladder as shown in Fig. 2(a). The

numerical results converge and are independent of the choices of subsystem in the thermal dynamic limit, $L \gg L_A \gg 1$. In Figs. 2(b) and 2(c), we show the entanglement spectra λ_α and entanglement entropy S_A obtained by calculating the Green's function from the effective Hamiltonian, Eq. (2). The topological regime for $\lambda_\alpha = 1/2$ appears through a topological phase transition at which the entanglement entropy diverges. In Fig. 2(d), we show the regime of topological nontrivial phase ($\lambda_\alpha = 1/2$), which is exactly the same regime as defined by Eq. (10). These numerical results agree with the analytic calculation of the winding number, confirming the topological properties in our current system.

B. Flat-band structure and edge state wave function

In our numerical calculation above, the topological properties of the Kitaev ladder (and hence the multilayer structure in our original proposal) have been confirmed in a periodic boundary condition along the normal (z) direction. However, the localized edge state wave function as well as the possible zero energy modes still have to be obtained within an open boundary condition.

In this section, we perform a full exact diagonalization on the mean-field Hamiltonian in Eq. (3), where a long-ranged order parameter (pairing) is included with an open boundary condition. In Fig. 3(a), we show the obtained single-particle energy as a function of the in-plane momentum $|\mathbf{k}_\parallel| = k_x$(we choose $k_y = 0$) for $\mu^* = \Delta^{(1)}_{\mathbf{k}_\parallel} = t_z^*$ with finite layer number $L = 100$.

The continuous energy bands above and below zero energy is the Bogoliubov excitation spectrum, while a new zero energy flat band appears between zero momentum and $k_{\rm Max} = \sqrt{2m^*(\mu^* + 2t_z^*)} = \sqrt{3}k_F$, where $k_F \equiv \sqrt{2m^*\mu^*} = \sqrt{2m^*t_z^*}$. In Fig. 3(a), due to the finite-size effect, the energy spectra split near the gap closed point.

From Bogoliubov excitation energies in Eq. (7), it is easy to show that the gap is closed at $k_x = k_{\rm Max}$, and $k_y = k_z = 0$.

The presence of such a zero energy flat-band structure indicates that the Majorana surface zero modes do exist in our current 3D system, while its topological properties are classified to be *BDI* class as a Kitaev chain.

We note that such quantum degenerate MSZMs have an overlapping wave function in the 2D surface, and therefore become a very interesting systems for investigating the many-body physics of non-Abelian particles. We will then discuss its stability in details in the next section.

When $\mu^* > 2t_z^*$, however, the physical properties are changed: there will be a ring structure in momentum space, where the Kitaev ladder becomes topological as $k_{\rm Min} < |\mathbf{k}_\parallel| < k_{\rm Max}$; see Eq. (10). In addition to the gapless ring as $|\mathbf{k}_\parallel| = k_{\rm Max}$, the Bogoliubov excitation energy gap also closes at $|\mathbf{k}_\parallel| = k_{\rm Min}$. However, different from previous case, the appearance of these new gapless rings may cause additional coupling between Majorana fermions and the Bogoliubov particles, making the topological phases unstable against local disorder potential. We will discuss this issue in the next section.

Besides the energy spectrum, in Fig. 3(b), we also show the density distribution, $\rho_j(\mathbf{k}_\parallel) \equiv \langle\psi^0_{\mathbf{k}_\parallel}|c^\dagger_{\mathbf{k}_\parallel,j}c_{\mathbf{k}_\parallel,j}|\psi^0_{\mathbf{k}_\parallel}\rangle$, for the Majorana zero modes along the normal direction (z direction). Here $|\psi^0_{\mathbf{k}_\parallel}\rangle$ is the single-particle wave function of the zero energy state for a given in-plane momentum, obtained by exactly diagonalizing the Bogoliubov Hamiltonian. We find that the wave function does decay more slowly than an exponential function inside the bulk, reflecting the effects of dipolar interaction when compared to the results of nearest-neighboring pairing only. Besides, the decay slope is directly related to the energy gap for a given in-plane momentum $\mathbf{k}_\parallel$. For example, the energy gap is largest near $\mathbf{k}_\parallel = k_F$, and the MF wave function decays with fast slope (shortest decay length). When $\mathbf{k}_\parallel$ is closed to $k_{\rm Max}$, that is, the energy gap is closing, the single-particle wave function of the zero energy state becomes long tailed, as expected.

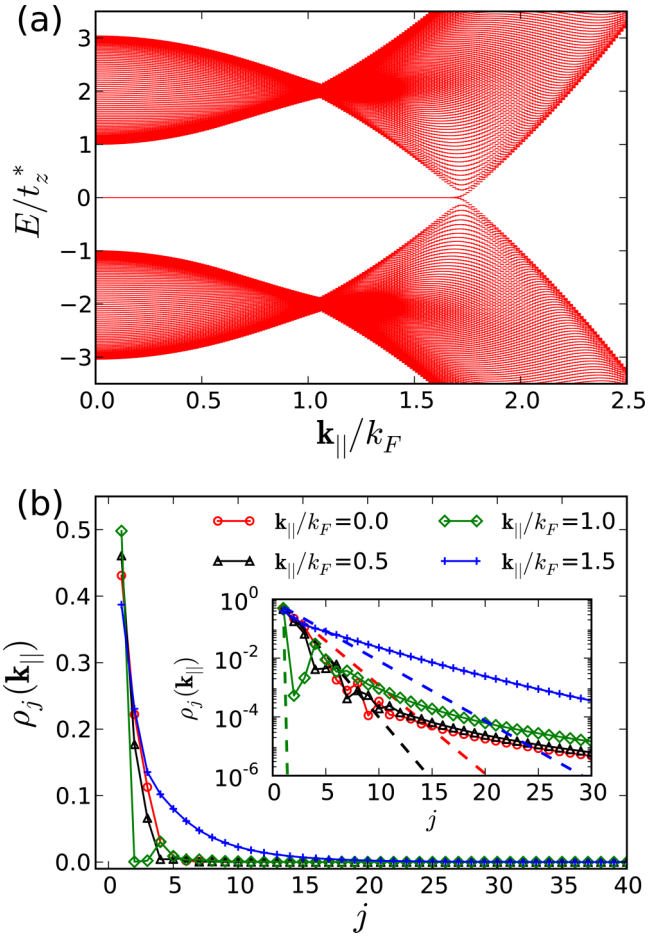

FIG. 3. (a) Single-particle band structure of ladder Hamiltonian [see Eq. (3)] obtained by exactly diagonalizing $L = 100$ layers with a long-ranged (dipolar) pairing for $\mu^* = \Delta^{(1)}_{\mathbf{k}_\parallel} = t_z^*$. (b) Particle density distribution $\rho_j(\mathbf{k}_\parallel)$ in the real space for the Majorana zero modes for different in-plane momentum $\mathbf{k}_\parallel$ with $\mu^* = \Delta^{(1)}_{\mathbf{k}_\parallel} = t_z^*$. Inset: Semilog plot for the same data. The dashed lines are results for nearest-neighboring pairing only.

V. STABILITY OF MSZMs

In this section, we discuss the stability of the unpaired MSZMs obtained from the Kitaev ladder in momentum space [see Eq. (3)]. There are two aspects to study: first, whether the system will be stable against the single-particle perturbation

on the edge surface; second, whether the system is stable against the possible interaction between Majorana fermions due to the dipolar interaction. We will verify the first by applying the time-reversal symmetry (TRS) on the current system, and argue the second from existing results in similar systems.

A. Stability with respect to disorder or inhomogeneous potential

In this paper, we concentrate on the situation when $\mu^* < 2t_z^*$ such that the 1D Kitaev ladders of *all* in-plane momentum are topological [see Fig. 3(a) and Eq. (10)]. The most general single-particle perturbation on these unpaired MFs in the bottom layer ($j = 1$) can be expressed as $H_{\rm dis} = H_1 + H_2$, where

$$H_1 = i \sum_{\mathbf{k}_\parallel \neq -\mathbf{k}'_\parallel} A(\mathbf{k}_\parallel, \mathbf{k}'_\parallel) \tilde{\gamma}^{(1)}_{\mathbf{k}_\parallel,1} \tilde{\gamma}^{(1)}_{\mathbf{k}'_\parallel,1},$$

$$H_2 = i \sum_{\mathbf{k}_\parallel} A(\mathbf{k}_\parallel, -\mathbf{k}_\parallel) \tilde{\gamma}^{(1)}_{\mathbf{k}_\parallel,1} \tilde{\gamma}^{(1)}_{-\mathbf{k}_\parallel,1}. \tag{13}$$

Here $A(\mathbf{k}_\parallel, \mathbf{k}'_\parallel)$ is a general single-particle potential due to local disorder or inhomogeneous potential $U_{\rm trap}(\mathbf{r}_\parallel)$ in the in-plane (x-y) direction. To avoid confusion, we also have defined all the unpaired MFs to be $\tilde{\gamma}^{(1)}_{\mathbf{k}_\parallel,1}$.

Note that these MF symbols are defined in momentum space and therefore has slightly different properties compared to the regular MFs defined in real space. As described in Appendix A, the MFs in momentum space have $(\tilde{\gamma}^{(1)}_{\mathbf{k}_\parallel,1})^\dagger = \tilde{\gamma}^{(1)}_{-\mathbf{k}_\parallel,1}$, $\mathcal{T}\tilde{\gamma}^{(1)}_{\mathbf{k}_\parallel,1}\mathcal{T}^{-1} = \tilde{\gamma}^{(1)}_{-\mathbf{k}_\parallel,1}$. They satisfy the exchange properties, $\{\tilde{\gamma}^{(1)}_{\mathbf{k}_\parallel,1}, \tilde{\gamma}^{(1)}_{\mathbf{k}'_\parallel,1}\} = 2\delta_{\mathbf{k}_\parallel,-\mathbf{k}'_\parallel}$. This is why we separate out terms with $\mathbf{k}'_\parallel = -\mathbf{k}_\parallel$ in the above definition.

Starting from the H_1 term, it is easy to find that the Hermitian property of H_1 leads to the following constraint:

$$A(\mathbf{k}_\parallel, \mathbf{k}'_\parallel) = A(-\mathbf{k}_\parallel, -\mathbf{k}'_\parallel)^*, \tag{14}$$

because

$$\begin{aligned} H_1 = H_1^\dagger &= -i \sum_{\mathbf{k}_\parallel \neq -\mathbf{k}'_\parallel} A(\mathbf{k}_\parallel, \mathbf{k}'_\parallel)^* \tilde{\gamma}^{(1)}_{-\mathbf{k}'_\parallel,1} \tilde{\gamma}^{(1)}_{-\mathbf{k}_\parallel,1} \\ &= i \sum_{\mathbf{k}_\parallel \neq -\mathbf{k}'_\parallel} A(\mathbf{k}_\parallel, \mathbf{k}'_\parallel)^* \tilde{\gamma}^{(1)}_{-\mathbf{k}_\parallel,1} \tilde{\gamma}^{(1)}_{-\mathbf{k}'_\parallel,1} \\ &= i \sum_{\mathbf{k}_\parallel \neq -\mathbf{k}'_\parallel} A(-\mathbf{k}_\parallel, -\mathbf{k}'_\parallel)^* \tilde{\gamma}^{(1)}_{\mathbf{k}_\parallel,1} \tilde{\gamma}^{(1)}_{\mathbf{k}'_\parallel,1}. \end{aligned} \tag{15}$$

On the other hand, the time-reversal symmetry (TRS) of the system leads to

$$A(\mathbf{k}_\parallel, \mathbf{k}'_\parallel) = -A(-\mathbf{k}_\parallel, -\mathbf{k}'_\parallel)^*, \tag{16}$$

because

$$\begin{aligned} H_1 &= \mathcal{T} H_1 \mathcal{T}^{-1} \\ &= -i \sum_{\mathbf{k}_\parallel \neq -\mathbf{k}'_\parallel} A(\mathbf{k}_\parallel, \mathbf{k}'_\parallel)^* \tilde{\gamma}^{(1)}_{-\mathbf{k}_\parallel,1} \tilde{\gamma}^{(1)}_{-\mathbf{k}'_\parallel,1} \\ &= -i \sum_{\mathbf{k}_\parallel \neq -\mathbf{k}'_\parallel} A(-\mathbf{k}_\parallel, -\mathbf{k}'_\parallel)^* \tilde{\gamma}^{(1)}_{\mathbf{k}_\parallel,1} \tilde{\gamma}^{(1)}_{\mathbf{k}'_\parallel,1}. \end{aligned} \tag{17}$$

One can see easily that the function $A(\mathbf{k}_\parallel, \mathbf{k}'_\parallel) = 0$ for all $\mathbf{k}'_\parallel \neq -\mathbf{k}_\parallel$, because Eqs. (14) and (16) cannot be satisfied simultaneously.

As for the remaining term, H_2, the Hermitian property requires that $A(\mathbf{k}_\parallel, -\mathbf{k}_\parallel) = -A(\mathbf{k}_\parallel, -\mathbf{k}_\parallel)^*$, because

$$H_2 = H_2^\dagger = -i \sum_{\mathbf{k}_\parallel} A(\mathbf{k}_\parallel, -\mathbf{k}_\parallel)^* \tilde{\gamma}^{(1)}_{\mathbf{k}_\parallel,1} \tilde{\gamma}^{(1)}_{-\mathbf{k}_\parallel,1}. \tag{18}$$

The TRS requires that $A(\mathbf{k}_\parallel, -\mathbf{k}_\parallel) = -A(-\mathbf{k}_\parallel, \mathbf{k}_\parallel)^*$, because

$$\begin{aligned} H_2 &= \mathcal{T} H_2 \mathcal{T}^{-1} \\ &= -i \sum_{\mathbf{k}_\parallel} A(\mathbf{k}_\parallel, -\mathbf{k}_\parallel)^* \tilde{\gamma}^{(1)}_{-\mathbf{k}_\parallel,1} \tilde{\gamma}^{(1)}_{\mathbf{k}_\parallel,1} \\ &= -i \sum_{\mathbf{k}_\parallel} A(-\mathbf{k}_\parallel, \mathbf{k}_\parallel)^* \tilde{\gamma}^{(1)}_{\mathbf{k}_\parallel,1} \tilde{\gamma}^{(1)}_{-\mathbf{k}_\parallel,1}. \end{aligned} \tag{19}$$

In other words, we obtain $A(\mathbf{k}_\parallel, -\mathbf{k}_\parallel) = A(-\mathbf{k}_\parallel, \mathbf{k}_\parallel)$. This implies that

$$\begin{aligned} H_2 &= i \sum_{\mathbf{k}_\parallel} A(\mathbf{k}_\parallel, -\mathbf{k}_\parallel) \tilde{\gamma}^{(1)}_{\mathbf{k}_\parallel,1} \tilde{\gamma}^{(1)}_{-\mathbf{k}_\parallel,1} \\ &= i \sum_{\mathbf{k}_\parallel} A(-\mathbf{k}_\parallel, \mathbf{k}_\parallel) \tilde{\gamma}^{(1)}_{\mathbf{k}_\parallel,1} \tilde{\gamma}^{(1)}_{-\mathbf{k}_\parallel,1} \\ &= i \sum_{\mathbf{k}_\parallel} A(\mathbf{k}_\parallel, -\mathbf{k}_\parallel) \tilde{\gamma}^{(1)}_{-\mathbf{k}_\parallel,1} \tilde{\gamma}^{(1)}_{\mathbf{k}_\parallel,1} \\ &= \frac{i}{2} \sum_{\mathbf{k}_\parallel \neq 0} A(\mathbf{k}_\parallel, -\mathbf{k}_\parallel) \big[\tilde{\gamma}^{(1)}_{\mathbf{k}_\parallel,1} \tilde{\gamma}^{(1)}_{-\mathbf{k}_\parallel,1} \\ &\quad + \tilde{\gamma}^{(1)}_{-\mathbf{k}_\parallel,1} \tilde{\gamma}^{(1)}_{\mathbf{k}_\parallel,1} \big] + iA(0,0) \tilde{\gamma}^{(1)}_{0,1} \tilde{\gamma}^{(1)}_{0,1} \\ &= i \sum_{\mathbf{k}_\parallel \neq 0} A(\mathbf{k}_\parallel, -\mathbf{k}_\parallel) + iA(0,0), \end{aligned} \tag{20}$$

which is nothing but a constant only.

Therefore, we find that *any* single-particle perturbation, $H_{\rm dis} = H_1 + H_2$, is actually irrelevant to the energy or wave-function Majorana fermions. This important consequence results from the fact that *all* unpaired MFs in the bottom layer, i.e., $\tilde{\gamma}^{(1)}_{\mathbf{k},1}$, are transformed in the same way under time-reversal operation, while the other type of Majorana fermion, $\tilde{\gamma}^{(2)}_{\mathbf{k},1}$, is not involved in this bottom layer at all. Therefore, the system composed by a single type of MF should be robust against any single-particle perturbation when the time-reversal symmetry is considered, at least within the mean-field approximation we consider in this paper. This important result also applies to inhomogeneous trapping potential in the in-plane (x-y) direction, since it can be always written in the same form as $H_{\rm dis}$ even without a periodic boundary condition.

Finally, we emphasize that the topological properties of the multilayer structure discussed in this paper can be also understood as a 2D array of Kitaev chains *in real space*, where the interchain tunneling makes the Majorana fermion mobile in the (x-y) plane. In fact, Wakatsuki, Ezawa, and Nagaosa in Ref. [20] have shown that the Majorana zero modes of their multichain system can still exist and are of multidegeneracy when interchain tunneling is turned on with an *open* boundary condition. In other words, the zero energy flat band does not

depend on the assumption of periodic potential, completely consistent with results derived above. However, since our analytic results are confirmed by investigating the equivalent Kitaev two-leg ladders in momentum space [see Fig. 1(b) and Eq. (2)], our approach can be easily generalized to the thermodynamic limit in a mesoscopic system.

B. Stability with respect to the coupling between MSZMs and Bogoliubov quasiparticles

The single-particle perturbation in $H_{\rm dis}$ discussed above includes the coupling between MSZMs only. In principle, the disorder potential may also couple MSZMs and Bogoliubov quasiparticles in the bulk. From a perturbation point of view, such coupling could be suppressed by the superfluid pairing gap, and the only possible nontrivial effects can appear only near the gapless ring: $|\mathbf{k}_\parallel| = k_{\rm Max}$.

However, we have to emphasize that the effects of such hybridization depends not only on the energy differences between particles, but also the occupation number in the relevant states. We will show that the occupation number of particles near the gapless ring at $|\mathbf{k}_\parallel| = k_{\rm Max}$ should be very small, and hence the coupling between MSZMs and the Bogoliubov quasiparticles should be also irrelevant to influence the topological properties.

In order to see this, we first calculate the in-plane occupation number of particles near $|\mathbf{k}_\parallel| = k_{\rm Max}$, which is the Fermi momentum at $k_z = 0$. Without loss of generality, the occupation number can be easily estimated by using periodic boundary condition. Within the standard BCS theory, the 3D occupation number in momentum space at zero temperature is given by $n^{3D}_{\mathbf{k}} = \frac{1}{2}[1 - \xi_{\mathbf{k}}/E^{(+)}_{\mathbf{k}}]$, where $E^{(+)}_{\mathbf{k}}$ is the Bogoliubov excitation energy in Eq. (7). Therefore the 2D occupation number of particles for a given in-plane momentum is given by

$$\begin{aligned} n^{2D}_{\mathbf{k}_\parallel} &\equiv \int_{-\pi/d}^{\pi/d} \frac{dk_z}{2\pi} n^{3D}_{\mathbf{k}} = \frac{1}{2}\int_{-\pi/d}^{\pi/d} \frac{dk_z}{2\pi}\left[1 - \frac{\xi_{\mathbf{k}}}{E^{(+)}_{\mathbf{k}}}\right] \\ &\sim \int_{-\pi/d}^{\pi/d} \frac{dk_z}{2\pi}\frac{1}{2}\left[1 - \frac{\xi_{\mathbf{k}}}{|\xi_{\mathbf{k}}|}\right] \\ &= \int_{-k_0}^{k_0} \frac{dk_z}{2\pi} = \frac{1}{\pi d}\cos^{-1}\left(\frac{\mathbf{k}^2_\parallel/2m^* - \mu^*}{2t^*_z}\right), \end{aligned} \tag{21}$$

where $k_0 \equiv \frac{1}{d}\cos^{-1}[(\mathbf{k}^2/2m^* - \mu^*)/2t^*_z]$. From the second line, we have assumed the gap is small and negligible compared to the chemical potential, so that a certain analytic estimate can be derived.

It is easy to see that $n^{2D}_{\mathbf{k}_\parallel} \to \frac{1}{\pi d}\cos^{-1}(1) = 0$, when $|\mathbf{k}_\parallel| \to k_{\rm Max} = \sqrt{2m^*(\mu^* + 2t^*_z)}$. In other words, we could reasonably expect that there is almost *no* Bogoliubov particles or Majorana fermions occupied near the gapless ring at $|\mathbf{k}_\parallel| = k_{\rm Max}$. Therefore, after considering the negligible occupation number of particles near the gapless ring, we believe it is reasonable to neglect the coupling between MSZMs and Bogoliubov quasiparticles. The topological system we proposed should be still stable in the thermal dynamic limit.

Finally, we note that when $\mu^* > 2t^*_z$, an additional gapless ring appears at $|\mathbf{k}_\parallel| = k_{\rm Min}$, where the occupation number there is still finite and like the case near $|\mathbf{k}_\parallel| = k_{\rm Max}$. As a result, a certain coupling between the Majorana surface modes and the Bogoliubov quasiparticles may be possible. The topological property for the latter case may still exist, but should be further investigated and is therefore not the situation we will consider in this paper.

The same may be said of the trapping potential. If the trapping potential is shallow so that the local-density approximation can be applied, we can treat this problem by replacing the chemical potential μ by a position dependent form, i.e., $\mu(r_\parallel) = \mu + \frac{1}{2}m^*\omega^2 r^2_\parallel$, where m^* is the effective mass of polar molecules and ω is the trapping frequency. As a result, we could still apply our analysis and obtain the regime for a topological phase by $|\mathbf{k}^2_\parallel/2m^* - \mu(r_\parallel)| < 2t^*_z$.

In other words, if only $\mu(r_\parallel) < 2t^*_z$, the whole system is still well protected as we have discussed: All the possible scattering between Bogoliubov quasiparticles in the bulk and the Majorana zero modes appear near the gapless regime, $k_{\rm Max} = \sqrt{2m^*[\mu(r_\parallel) + 2t_z]}$.

However, as we have shown in Eq. (21), the occupation number of Bogoliubov quasiparticles near the gapless regime is also negligible.

Such a kind of inhomogeneous potential has been actually studied for an array of 1D Kitaev chains in Ref. [20]. They also numerically show that the zero modes could still exist and are stable for such a case (with a finite trapping potential). Therefore, we believe that the trapping potential should not affect the stability of the topological phases we proposed here, if only the local chemical potential is not too large [i.e., $\mu(r_\parallel) = \mu + \frac{1}{2}m^*\omega^2 r^2_\parallel < 2t^*_z$].

C. Stability with respect to in-plane repulsive interaction

In this section, we briefly address the interaction effects between MSZMs. We start by considering results in both high-density and low-density regimes, where the pairing is better defined in the real space for the former, while it is better defined in momentum space for the latter. We will argue that they should exhibit the same topological phase even in the intermediate regime at least within the mean-field approximation. Full analytic or numerical calculation beyond the mean-field level is beyond the scope of this paper and should be studied more carefully in the future.

Our argument starts from the high-density limit (not addressed in this paper), where the averaged interparticle distance between polar molecules in the same layer is shorter than the interlayer spacing. Hence the horizontal (in-plane) kinetic energy is suppressed by the strong repulsive dipolar interaction. As a result, polar molecules in each layer can be self-assembled to be a triangular lattice, and the relative position of these lattice points (molecules) are mostly frozen and aligned to each other [see Fig. 4(a) and Refs. [51,63]].

When a small amount of vacancies appears for certain chemical potential, p-wave superfluidity appears within each 1D chain along the normal (z) direction, and the system becomes almost equivalent to a planar array of 1D Kitaev chains.

The topological properties therefore should be equivalent to a 2D array of Kitaev chain with interlayer pairing, i.e., the *BDI* class (as the regular Kitaev chain) with localized

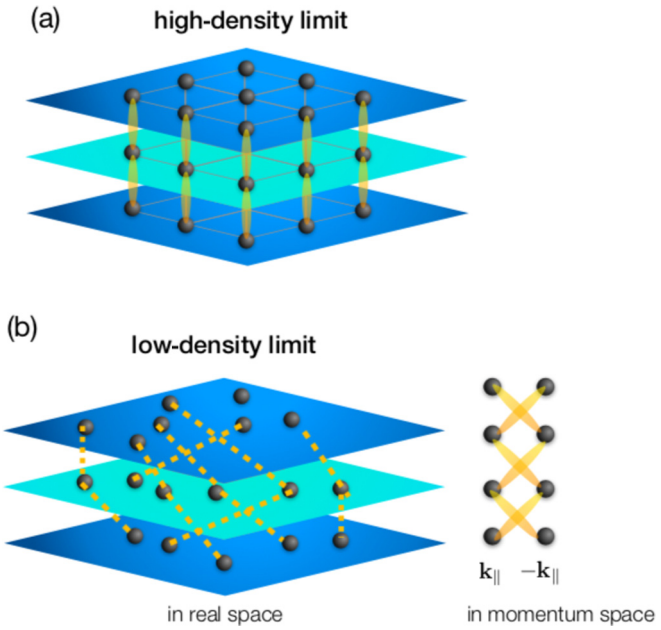

FIG. 4. Schematic plots of polar molecules in a multilayer system in high-density limit (a) and in low-density limit (b) respectively. In high-density limit, strong repulsive dipolar interaction makes the molecules form a triangular crystal in each layer. On the other hand, in low-density limit, molecules are free-moving without fixed relative position to each other. Therefore when interlayer attraction is increased by reducing interlayer distance, the former can form a 2D array of Kitaev chains with a vertical pairing between each other in different layers, while the latter will form cross pairing between in-plane momenta $\mathbf{k}_\parallel$ and $-\mathbf{k}_\parallel$ as in a Kitaev ladder [see also Fig. 1(b), Eqs. (2) and (3)]. Here for simplicity, we just show the pairing between molecules in the nearest-neighboring layers (denoted by yellow elliptical curves) and use dashed line to demonstrate the (schematic) paring in real space.

Majorana fermions at the edge forming a flat band as studied in Ref. [20].

In the dilute limit (which is what we studied in this paper), the intralayer dipolar repulsion is actually much weaker compared to the in-plane kinetic energy. It is well justified to apply Landau-Fermi-liquid theory in each 2D layer before the interlayer pairing is introduced (see Refs. [39,53]). Such a weak intralayer repulsion just renormalizes the effective mass and chemical potential, and the topological properties of such a multilayer system can be understood as a bundle of 1D Kitaev ladder in momentum space, as we addressed in the previous part of this paper. The resulting topological phase also belongs to the *BDI* class with quantum degenerate Majorana surface modes in the top and bottom layer if Eq. (10) is satisfied; see Fig. 4(b). The second-order (induced) interaction [64] is relatively much weaker than the direction dipole-dipole interaction in the dilute limit, and therefore we will not consider it in our present calculation.

In the middle range of the in-plane density, however, intralayer repulsion is comparable to the in-plane kinetic energy and hence the topological properties have to be identified beyond the single-particle (mean-field) picture. A relevant study on the interaction effects of Majorana fermions has been discussed [65,66]. For example, Fidkowski and Kitaev have shown that the *BDI* class with $\mathbb{Z}$ topological invariance shall be broken to $\mathbb{Z}_8$ when a short-ranged four-point interaction is included [65,66].

But we note that in our present system the long-ranged nature of dipolar interaction also makes the system quite different from the short-ranged case studied by Fidkowski and Kitaev. More specifically, we could write down the most general mutual interaction term between four fermions in the bottom layers to be

$$H_\gamma = \frac{1}{\Omega}\sum_{\mathbf{k}_{\parallel,i}}{}' U_\gamma(\{\mathbf{k}_{\parallel,i}\})\tilde{\gamma}^{(1)}_{\mathbf{k}_{\parallel,1},1}\tilde{\gamma}^{(1)}_{\mathbf{k}_{\parallel,2},1}\tilde{\gamma}^{(1)}_{\mathbf{k}_{\parallel,3},1}\tilde{\gamma}^{(1)}_{\mathbf{k}_{\parallel,4},1}, \quad (22)$$

where $U_\gamma(\mathbf{k}_{\parallel,1},\ldots,\mathbf{k}_{\parallel,4})$ is some complicated interaction matrix element between MFs, $\tilde{\gamma}^{(1)}_{\mathbf{k}_{\parallel,i},1}$. $\sum'_{\mathbf{k}_{\parallel,i}}$ indicates a summation of $\mathbf{k}_{\parallel,i}$ with the conservation of total momentum, $\mathbf{k}_{\parallel,1}+\cdots+\mathbf{k}_{\parallel,4}=0$.

In order to recover Fidkowski and Kitaev's result for Z_8 symmetry, U_γ has to be a constant, independent of the in-plane momenta. This indicates that the bare interaction between polar molecules has to be a short-ranged interaction in the real space, which cannot be realistic or effective for our spinless fermionic polar molecules. In fact, fermionic SPT phases are not totally understood yet in 3D system, although it is argued that there exists a bulk SPT and surface symmetry enriched TO anomaly matching in a 3D bosonic weak SPT phase [3]. It is a very interesting and challenging subject for future study. The multilayer structure as well as the Majorana surface modes proposed in this paper suggest a very promising system to investigate the many-body physics of these non-Abelian particles.

Finally, we note that in Ref. [20] the authors also studied the case when the interchain pairing is included. Within the mean-field (BCS) approximation, they find that the multidegenerate Majorana zero modes are still present and stable if the interchain pairing is of the same phase as the intrachain pairing. These degenerate zero modes become unstable (and hence with a finite dispersion) *only* when the time-reversal symmetry is broken (i.e., the interchain pairing is of a different phase than the intrachain pairing). Therefore, it is reasonable to expect that the quantum degenerate Majorana surface zero modes (in the *BDI* class) observed in our multilayer system may be still stable against the in-plane repulsive interaction between polar molecules, where the time-reversal symmetry is still strictly preserved.

VI. EXPERIMENTAL MEASUREMENT

There have been several proposals to measure MFs. The simplest way is by observing the long-distance correlation between MFs in the two ending layers (for example, see [67]), which should cause a short interference period [i.e., $\propto\cos(k_z Ld)$] in momentum space (i.e., in the long-time approximation of the time-of-flight experiments). Here Ld is the distance between the top and bottom layers. We emphasize that such measurement for the 1D Kitaev chain model suffers a serious noise-to-signal ratio [67], since only "one" Majorana mode exists at each end of the chain. Besides, the fact that no long-ranged order can exist in 1D system also makes it

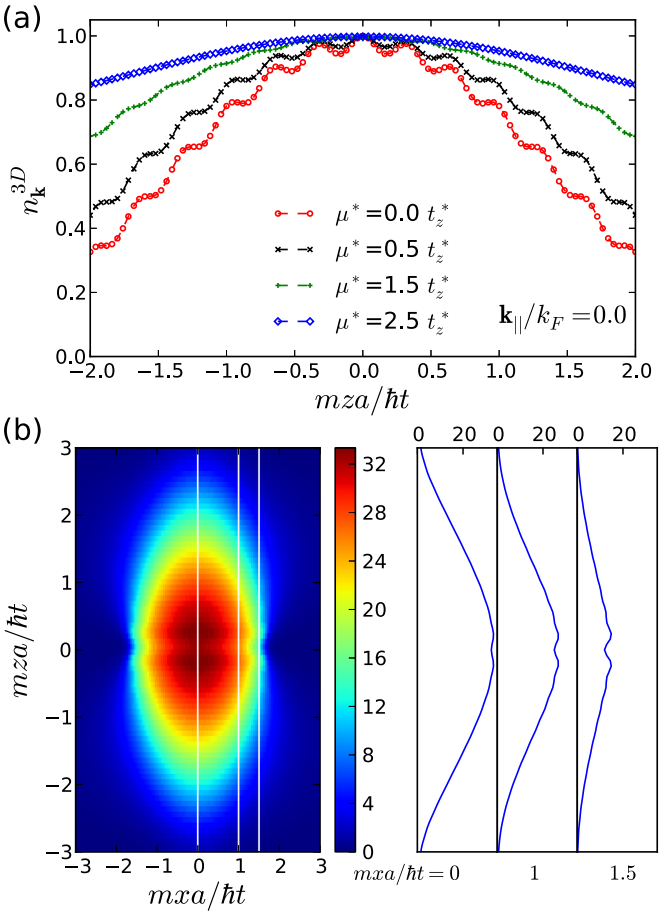

FIG. 5. (a) The momentum distribution in 3D space $n_{\mathbf{k}}^{3D}$ as a function of the final position z with fixed $\mathbf{k}_\parallel/k_F = 0$ for various μ^*. (b) Integrated momentum distribution along y direction, $n_{\mathrm{ToF}}(x, z)$, for time-of-flight measurement, showing a possible feature on the interference pattern in the time-of-flight experiment. Here we consider $\mu^* = \Delta_{\mathbf{k}_\parallel}^{(1)} = t_z^*$. The three cross sections ($mx/\hbar t = 0, 1, 1.5$) at different horizontal direction are shown on the right.

difficult to expect a significant signal. In our multilayer system, however, unpaired MFs are macroscopically degenerate near the surface layers, and therefore the experimental measurement of these MSZMs becomes much more promising.

The unpaired MFs can be characterized by the nonlocal fermionic correlations which can be detected in time-of-flight (ToF) imaging, as illustrated in Fig. 5. We then study the time-of-flight image for a free expansion time t, obtained by integrating over the y direction, i.e.,

$$n_{\mathrm{ToF}}(x, z) \propto \left|\tilde{\omega}_0\left(\frac{mz}{\hbar t}\right)\right|^2 \int_{-\infty}^{\infty} dy\, n^{3D}_{m\mathbf{r}/\hbar t}, \tag{23}$$

where the final position $\mathbf{r} = \hbar\mathbf{k}t/m$, and $\tilde{\omega}_0(k_z)$ is the fourier transform of the lowest band Wannier function. $n_{\mathbf{k}}^{3D}$ is the momentum distribution in 3D space,

$$n_{\mathbf{k}}^{3D} = n^{3D}_{\mathbf{k}_\parallel, k_z} \equiv \sum_{j,j'=1}^{L} \langle G|c^\dagger_{\mathbf{k}_\parallel, j} c_{\mathbf{k}_\parallel, j'}|G\rangle\, e^{i(j-j')dk_z}, \tag{24}$$

where $|G\rangle$ is the ground-state wave function obtained by diagonalizing the mean-field Hamiltonian in Eq. (2) with a long-ranged pairing.

We first calculate the momentum distribution $n_{\mathbf{k}}^{3D}$ with fixed in-plane momentum $\mathbf{k}_\parallel = 0$ with various chemical potentials. By ramping the chemical potential, we can detect the transition point, since the oscillations disappear if we approach the transition point at $\mu^* = 2t_z^*$ [see Fig. 5(a)] with $\mathbf{k}_\parallel/k_F = 0$. This numerical result agrees with Eq. (10). In Fig. 5(b), we show the TOF signals for the case with $\mu^* = \Delta_{\mathbf{k}_\parallel}^{(1)} = t_z^*$, proving that the oscillations will still be present in the topological regime. As we can see, when the system is in the topological regime, additional interference fringes emerge due to the long-ranged correlation between macroscopically degenerate Majorana surface modes in the top and bottom layers. The contrast of such interference to its average density is larger when away from the center, making it possible to be measured in the present experiments.

VII. CONCLUSION

In this paper, we propose that a topological state can be prepared and observed in a stack of 2D layers with fermionic polar molecules polarized to the normal direction. The associated quantum degenerate Majorana surface modes appear in the surface layers due to the 3D p-wave superfluidity, confirmed by the winding number, entanglement spectrum, and entanglement entropy numerics. We also show the parameter regime to find MFs in the current experiments. Our work paves the way for future investigation of the many-body physics with non-Abelian statistics under time-reversal symmetry.

ACKNOWLEDGMENTS

We thank C.-Y. Mou, S.-J. Huang, Y.-P. Huang, J.-S. You, and G. Juzeliunas for valuable discussions.

APPENDIX A: EXACT SOLUTION FOR A SPECIAL CASE OF KITAEV LADDER IN MOMENTUM SPACE

In this section, we will derive the exact solution for a special case of Kitaev ladder in momentum space, i.e., $\mu^* - \mathbf{k}_\parallel^2/2m^* = 0$ and $\Delta_{\mathbf{k}_\parallel}^{(1)} = t_z^*$ in Eq. (2). All longer-ranged pairing is assumed to be zero for simplicity.

1. Majorana fermions in momentum space

To see how MFs appear in $H_{\mathbf{k}_\parallel}^{\mathrm{ladd}}$, we first note that the definition of Majorana fermions (MFs) in real space is different from those in momentum space. For a general fermionic field operator $C(x)$ at the position x, its relation with MF operator $\Gamma(x)$ is the following:

$$C(x) = \tfrac{1}{2}[\Gamma_1(x) + i\Gamma_2(x)], \quad C^\dagger(x) = \tfrac{1}{2}[\Gamma_1(x) - i\Gamma_2(x)], \tag{A1}$$

and hence

$$\Gamma_1(x) = C(x) + C^\dagger(x), \quad \Gamma_2(x) = -i[C(x) - C^\dagger(x)]. \quad \text{(A2)}$$

Therefore, by doing Fourier transformation, the Majorana operators in momentum space can be given:

$$\Gamma_{1,k} = \int \Gamma_1(x) e^{-ikx} dx = \int C(x) e^{-ikx} dx + \int C^\dagger(x) e^{-ikx} dx = C_k + C^\dagger_{-k}, \quad \text{(A3)}$$

$$\Gamma_{2,k} = -i[C_k - C^\dagger_{-k}]. \quad \text{(A4)}$$

We note that now the MF operators $\Gamma_{1/2,k}$ are composed by the Dirac fermionic operator at momentum k and its antiparticles in the momentum $-k$.

From the above definition, the Hermitian and time-reversal operation of the Majorana fermions in momentum space become

$$\Gamma^\dagger_{1,k} = C^\dagger_k + C_{-k} = \Gamma_{1,-k}, \quad \text{(A5)}$$

$$\Gamma^\dagger_{2,k} = i[C^\dagger_k - C_{-k}] = \Gamma_{2,-k}, \quad \text{(A6)}$$

$$\mathcal{T}\,\Gamma_{1,k}\mathcal{T}^{-1} = C^\dagger_{-k} + C_k = \Gamma_{1,-k}, \quad \text{(A7)}$$

$$\mathcal{T}\,\Gamma_{2,k}\mathcal{T}^{-1} = i[C_{-k} - C^\dagger_k] = -\Gamma_{2,-k}, \quad \text{(A8)}$$

where $\mathcal{T}$ is the time-reversal operator. We have used the fact that $\mathcal{T}C(x)\mathcal{T}^{-1} = C(x)$ and $\mathcal{T}C_k\mathcal{T}^{-1} = C_{-k}$ to preserve the time-reversal symmetry.

2. The Hamiltonian in Majorana fermion basis

Using similar notation, we can define MFs in our present case as follows:

$$c_{\mathbf{k}_\parallel,j} = \tfrac{1}{2}\big[\gamma^{(1)}_{\mathbf{k}_\parallel,j} + i\,\gamma^{(2)}_{\mathbf{k}_\parallel,j}\big],\ c^\dagger_{\mathbf{k}_\parallel,j} = \tfrac{1}{2}\big[\gamma^{(1)}_{-\mathbf{k}_\parallel,j} - i\,\gamma^{(2)}_{-\mathbf{k}_\parallel,j}\big],\ c_{-\mathbf{k}_\parallel,j} = \tfrac{1}{2}\big[\gamma^{(1)}_{-\mathbf{k}_\parallel,j} + i\,\gamma^{(2)}_{-\mathbf{k}_\parallel,j}\big],\ c^\dagger_{-\mathbf{k}_\parallel,j} = \tfrac{1}{2}\big[\gamma^{(1)}_{\mathbf{k}_\parallel,j} - i\,\gamma^{(2)}_{\mathbf{k}_\parallel,j}\big] \quad \text{(A9)}$$

Since we are considering a special case, $\Delta_{\mathbf{k}_\parallel} = t_z^*$ and $\mathbf{k}_\parallel^2/2m^* = \mu^*$, the Hamiltonian in Eq. (2) can then be written as (here we consider nearest pairing $\Delta_{\mathbf{k}_\parallel} \equiv \Delta^{(1)}_{\mathbf{k}_\parallel}$ only and assume longer-ranged pairing, $\Delta^{(j)}_{\mathbf{k}_\parallel} = 0$ for $j > 1$)

$$H^{\text{ladd}}_{\mathbf{k}_\parallel} = -t_z \sum_{j=1}^{L-1} [c^\dagger_{\mathbf{k}_\parallel,j} c_{\mathbf{k}_\parallel,j+1} + c^\dagger_{-\mathbf{k}_\parallel,j} c_{-\mathbf{k}_\parallel,j+1} + c^\dagger_{\mathbf{k}_\parallel,j} c^\dagger_{-\mathbf{k}_\parallel,j+1} + c^\dagger_{-\mathbf{k}_\parallel,j} c^\dagger_{\mathbf{k}_\parallel,j+1} + c^\dagger_{\mathbf{k}_\parallel,j+1} c_{\mathbf{k}_\parallel,j} + c^\dagger_{-\mathbf{k}_\parallel,j+1} c_{-\mathbf{k}_\parallel,j} + c_{-\mathbf{k}_\parallel,j+1} c_{\mathbf{k}_\parallel,j} + c_{\mathbf{k}_\parallel,j+1} c_{-\mathbf{k}_\parallel,j},\ ], \quad \text{(A10)}$$

where L is the number of site or layers along the z direction.

After some straightforward algebra, the first four terms in the [ ] of the Hamiltonian are given by

$$\begin{aligned}
&\frac{1}{4}\big(\gamma^{(1)}_{-\mathbf{k}_\parallel,j} - i\,\gamma^{(2)}_{-\mathbf{k}_\parallel,j}\big)\big(\gamma^{(1)}_{\mathbf{k}_\parallel,j+1} + i\,\gamma^{(2)}_{\mathbf{k}_\parallel,j+1}\big) + \frac{1}{4}\big(\gamma^{(1)}_{\mathbf{k}_\parallel,j} - i\,\gamma^{(2)}_{\mathbf{k}_\parallel,j}\big)\big(\gamma^{(1)}_{-\mathbf{k}_\parallel,j+1} + i\,\gamma^{(2)}_{-\mathbf{k}_\parallel,j+1}\big) \\
&\quad + \frac{1}{4}\big(\gamma^{(1)}_{-\mathbf{k}_\parallel,j} - i\,\gamma^{(2)}_{-\mathbf{k}_\parallel,j}\big)\big(\gamma^{(1)}_{\mathbf{k}_\parallel,j+1} - i\,\gamma^{(2)}_{\mathbf{k}_\parallel,j+1}\big) + \frac{1}{4}\big(\gamma^{(1)}_{\mathbf{k}_\parallel,j} - i\,\gamma^{(2)}_{\mathbf{k}_\parallel,j}\big)\big(\gamma^{(1)}_{-\mathbf{k}_\parallel,j+1} - i\,\gamma^{(2)}_{-\mathbf{k}_\parallel,j+1}\big) \\
&= \frac{1}{4}\big(\gamma^{(1)}_{-\mathbf{k}_\parallel,j}\gamma^{(1)}_{\mathbf{k}_\parallel,j+1} + \gamma^{(2)}_{-\mathbf{k}_\parallel,j}\gamma^{(2)}_{\mathbf{k}_\parallel,j+1}\big) + \frac{i}{4}\big(\gamma^{(1)}_{-\mathbf{k}_\parallel,j}\gamma^{(2)}_{\mathbf{k}_\parallel,j+1} - \gamma^{(2)}_{-\mathbf{k}_\parallel,j}\gamma^{(1)}_{\mathbf{k}_\parallel,j+1}\big) \\
&\quad + \frac{1}{4}\big(\gamma^{(1)}_{\mathbf{k}_\parallel,j}\gamma^{(1)}_{-\mathbf{k}_\parallel,j+1} + \gamma^{(2)}_{\mathbf{k}_\parallel,j}\gamma^{(2)}_{-\mathbf{k}_\parallel,j+1}\big) + \frac{i}{4}\big(\gamma^{(1)}_{\mathbf{k}_\parallel,j}\gamma^{(2)}_{-\mathbf{k}_\parallel,j+1} - \gamma^{(2)}_{\mathbf{k}_\parallel,j}\gamma^{(1)}_{-\mathbf{k}_\parallel,j+1}\big) \\
&\quad + \frac{1}{4}\big(\gamma^{(1)}_{-\mathbf{k}_\parallel,j}\gamma^{(1)}_{\mathbf{k}_\parallel,j+1} - \gamma^{(2)}_{-\mathbf{k}_\parallel,j}\gamma^{(2)}_{\mathbf{k}_\parallel,j+1}\big) + \frac{-i}{4}\big(\gamma^{(1)}_{-\mathbf{k}_\parallel,j}\gamma^{(2)}_{\mathbf{k}_\parallel,j+1} + \gamma^{(2)}_{-\mathbf{k}_\parallel,j}\gamma^{(1)}_{\mathbf{k}_\parallel,j+1}\big) \\
&\quad + \frac{1}{4}\big(\gamma^{(1)}_{\mathbf{k}_\parallel,j}\gamma^{(1)}_{-\mathbf{k}_\parallel,j+1} - \gamma^{(2)}_{\mathbf{k}_\parallel,j}\gamma^{(2)}_{-\mathbf{k}_\parallel,j+1}\big) + \frac{-i}{4}\big(\gamma^{(1)}_{\mathbf{k}_\parallel,j}\gamma^{(2)}_{-\mathbf{k}_\parallel,j+1} + \gamma^{(2)}_{\mathbf{k}_\parallel,j}\gamma^{(1)}_{-\mathbf{k}_\parallel,j+1}\big). \quad \text{(A11)}
\end{aligned}$$

Similarly, the last four terms in the [ ] are given by

$$\begin{aligned}
&\frac{1}{4}\big(\gamma^{(1)}_{-\mathbf{k}_\parallel,j+1} - i\,\gamma^{(2)}_{-\mathbf{k}_\parallel,j+1}\big)\big(\gamma^{(1)}_{\mathbf{k}_\parallel,j} + i\,\gamma^{(2)}_{\mathbf{k}_\parallel,j}\big) + \frac{1}{4}\big(\gamma^{(1)}_{\mathbf{k}_\parallel,j+1} - i\,\gamma^{(2)}_{\mathbf{k}_\parallel,j+1}\big)\big(\gamma^{(1)}_{-\mathbf{k}_\parallel,j} + i\,\gamma^{(2)}_{-\mathbf{k}_\parallel,j}\big) \\
&\quad + \frac{1}{4}\big(\gamma^{(1)}_{-\mathbf{k}_\parallel,j+1} + i\,\gamma^{(2)}_{-\mathbf{k}_\parallel,j+1}\big)\big(\gamma^{(1)}_{\mathbf{k}_\parallel,j} + i\,\gamma^{(2)}_{\mathbf{k}_\parallel,j}\big) + \frac{1}{4}\big(\gamma^{(1)}_{\mathbf{k}_\parallel,j+1} + i\,\gamma^{(2)}_{\mathbf{k}_\parallel,j+1}\big)\big(\gamma^{(1)}_{-\mathbf{k}_\parallel,j} + i\,\gamma^{(2)}_{-\mathbf{k}_\parallel,j}\big) \\
&= \frac{1}{4}\big(\gamma^{(1)}_{-\mathbf{k}_\parallel,j+1}\gamma^{(1)}_{\mathbf{k}_\parallel,j} + \gamma^{(2)}_{-\mathbf{k}_\parallel,j+1}\gamma^{(2)}_{\mathbf{k}_\parallel,j}\big) + \frac{i}{4}\big(\gamma^{(1)}_{-\mathbf{k}_\parallel,j+1}\gamma^{(2)}_{\mathbf{k}_\parallel,j} - \gamma^{(2)}_{-\mathbf{k}_\parallel,j+1}\gamma^{(1)}_{\mathbf{k}_\parallel,j}\big) \\
&\quad + \frac{1}{4}\big(\gamma^{(1)}_{\mathbf{k}_\parallel,j+1}\gamma^{(1)}_{-\mathbf{k}_\parallel,j} + \gamma^{(2)}_{\mathbf{k}_\parallel,j+1}\gamma^{(2)}_{-\mathbf{k}_\parallel,j}\big) + \frac{i}{4}\big(\gamma^{(1)}_{\mathbf{k}_\parallel,j+1}\gamma^{(2)}_{-\mathbf{k}_\parallel,j} - \gamma^{(2)}_{\mathbf{k}_\parallel,j+1}\gamma^{(1)}_{-\mathbf{k}_\parallel,j}\big)
\end{aligned}$$

$$+\frac{1}{4}\left(\gamma^{(1)}_{-\mathbf{k}_\parallel,j+1}\gamma^{(1)}_{\mathbf{k}_\parallel,j}-\gamma^{(2)}_{-\mathbf{k}_\parallel,j+1}\gamma^{(2)}_{\mathbf{k}_\parallel,j}\right)+\frac{i}{4}\left(\gamma^{(1)}_{-\mathbf{k}_\parallel,j+1}\gamma^{(2)}_{\mathbf{k}_\parallel,j}+\gamma^{(2)}_{-\mathbf{k}_\parallel,j+1}\gamma^{(1)}_{\mathbf{k}_\parallel,j}\right)$$
$$+\frac{1}{4}\left(\gamma^{(1)}_{\mathbf{k}_\parallel,j+1}\gamma^{(1)}_{-\mathbf{k}_\parallel,j}-\gamma^{(2)}_{\mathbf{k}_\parallel,j+1}\gamma^{(2)}_{-\mathbf{k}_\parallel,j}\right)+\frac{i}{4}\left(\gamma^{(1)}_{\mathbf{k}_\parallel,j+1}\gamma^{(2)}_{-\mathbf{k}_\parallel,j}+\gamma^{(2)}_{\mathbf{k}_\parallel,j+1}\gamma^{(1)}_{-\mathbf{k}_\parallel,j}\right). \tag{A12}$$

Now using the anticommutation relations, $\{\gamma^{(a)}_{j,\mathbf{k}_\parallel},\gamma^{(b)}_{j',\mathbf{k}'_\parallel}\}=2\delta_{j,j'}\delta_{a,b}\delta_{\mathbf{k}_\parallel,-\mathbf{k}'_\parallel}$ $(a,b=1,2)$, we can obtain the Hamiltonian with special case $\Delta_{\mathbf{k}_\parallel}=t_z$,

$$H^{\text{ladd}}_{\mathbf{k}_\parallel}=it_z\sum_{j=1}^{L-1}\left(\gamma^{(2)}_{\mathbf{k}_\parallel,j}\gamma^{(1)}_{-\mathbf{k}_\parallel,j+1}+\gamma^{(2)}_{-\mathbf{k}_\parallel,j}\gamma^{(1)}_{\mathbf{k}_\parallel,j+1}\right). \tag{A13}$$

APPENDIX B: *BDI* CLASS AND WINDING NUMBER

In order to specify the TO, we have to check the symmetry first:

$$\mathcal{T}H(\mathbf{k})\mathcal{T}^{-1}=H(-\mathbf{k}),\mathcal{C}H(\mathbf{k})\mathcal{C}^{-1}=-H(-\mathbf{k}),\mathcal{S}H(\mathbf{k})\mathcal{S}^{-1}=-H(\mathbf{k}). \tag{B1}$$

Where $\mathcal{T}$, $\mathcal{C}$, and $\mathcal{S}$ are the antiunitary time-reversal symmetry (complex conjugate for the spinless model), particle-hole symmetry, and chiral symmetry (product of $\mathcal{T}$ and $\mathcal{C}$). It belongs to the *BDI* class and the topological phase is characterized by the $\mathbb{Z}$ index. This topological state is protected by chiral symmetry.

The BdG Hamiltonian can be unitary transformed to the off-diagonal form,

$$H_{\text{BdG}}=\frac{i}{4}\sum_{\mathbf{k}}\Gamma^\dagger_{\mathbf{k}}\begin{bmatrix}0 & v_{\mathbf{k}}\\ v^\dagger_{\mathbf{k}} & 0\end{bmatrix}\Gamma_{\mathbf{k}},$$

where $\mu^*_{\mathbf{k}_\parallel}=\mu^*+\frac{k^2_\parallel}{2m^*}$, $v_{\mathbf{k}}=-\mu^*_{\mathbf{k}_\parallel}-2t^*_z\cos(k_zd)-2i\Delta\sin(k_zd)$ and $v_{\mathbf{k}}=R(\mathbf{k})e^{i\theta(\mathbf{k})}$. Then, the corresponding Q matrix can be given,

$$Q_{\mathbf{k}}=\begin{bmatrix}0 & q_{\mathbf{k}}\\ q^\dagger_{\mathbf{k}} & 0\end{bmatrix},$$

where $q_{\mathbf{k}}=\frac{v_{\mathbf{k}}}{|v_{\mathbf{k}}|}=e^{i\theta_{\mathbf{k}}}$. The relevant space is the $U(N)$ unitary group. $q_{\mathbf{k}}$ is a mapping from the z direction BZ to $U(N)$, which is topologically classified by the first homotopy group, $\Pi_1[U(N)]=\mathbb{Z}$, characterized by the winding number W; see Ref. [2]. The winding number can be calculated as follows:

$$\begin{aligned}W_{\mathbf{k}_\parallel}&\equiv\int_{-\pi/d}^{\pi/d}\frac{dk_z}{2\pi}\partial_{k_z}\theta_{\mathbf{k}_\parallel,k_z}=\int_{-\pi/d}^{\pi/d}\frac{dk_z}{2\pi}\frac{\partial_{k_z}[-\cos\theta_{\mathbf{k}_\parallel,k_z}]}{\sin\theta_{\mathbf{k}_\parallel,k_z}}=\int_{-\pi/d}^{\pi/d}\frac{dk_z}{-2\pi}\frac{\partial_{k_z}\{-[\mu_{\mathbf{k}_\parallel}+2t_z\cos(k_zd)]/R(\mathbf{k})\}}{-[2\Delta_{\mathbf{k}_\parallel}\sin(k_zd)]}/R(\mathbf{k})\\&=\frac{1}{4\pi}\int_{-\pi}^{\pi}dk_z\frac{1}{\Delta_{\mathbf{k}_\parallel}\sin k_z}\left[2t_z\sin k_z+2\frac{[\mu_{\mathbf{k}_\parallel}+2t_z\cos k_z]}{R(\mathbf{k})^2}\left[2\Delta^2_{\mathbf{k}_\parallel}\sin k_z\cos k_z-t_z\sin k_z(\mu_{\mathbf{k}_\parallel}+2t_z\cos k_z)\right]\right]\\&=\frac{1}{2\pi\,\Delta_{\mathbf{k}_\parallel}}\int_{-\pi}^{\pi}dk_z\frac{4\Delta^2_{\mathbf{k}_\parallel}t_z+2\Delta^2_{\mathbf{k}_\parallel}\mu_{\mathbf{k}_\parallel}\cos k_z}{[\mu_{\mathbf{k}_\parallel}+2t_z\cos k_z]^2+4\Delta^2_{\mathbf{k}_\parallel}\sin^2k_z}.\end{aligned} \tag{B2}$$

Changing the variables $z=e^{ik_zd}$ and letting $J_1=\frac{t_z+\Delta_{\mathbf{k}_\parallel}}{\mu_{\mathbf{k}_\parallel}}$, $J_2=\frac{t_z-\Delta_{\mathbf{k}_\parallel}}{\mu_{\mathbf{k}_\parallel}}$, and $J_\pm=J_1\pm J_2$,

$$\begin{aligned}W_{\mathbf{k}_\parallel}&=\frac{1}{2\pi i}\oint\frac{dz}{z}\Delta_{\mathbf{k}_\parallel}\frac{4t_z+\mu_{\mathbf{k}_\parallel}\left(z+\frac{1}{z}\right)}{\left[\mu_{\mathbf{k}_\parallel}+t_z\left(z+\frac{1}{z}\right)\right]^2-\Delta^2_{\mathbf{k}_\parallel}\left(z-\frac{1}{z}\right)^2}\\&=\frac{\Delta_{\mathbf{k}_\parallel}}{2\pi i}\oint dz\frac{\mu_{\mathbf{k}_\parallel}z^2+4t_zz+\mu_{\mathbf{k}_\parallel}}{[(t_z+\Delta_{\mathbf{k}_\parallel})z^2+\mu_{\mathbf{k}_\parallel}z+(t_z-\Delta_{\mathbf{k}_\parallel})][(t_z-\Delta_{\mathbf{k}_\parallel})z^2+\mu_{\mathbf{k}_\parallel}z+(t_z+\Delta_{\mathbf{k}_\parallel})]}\\&=\frac{J_-}{2}\oint\frac{dz}{2\pi i}\frac{z^2+2J_+z+1}{[J_1z^2+z+J_2][J_2z^2+z+J_1]}\\&=\frac{J_-}{2}\oint\frac{dz}{2\pi i}\frac{z^2+2J_+z+1}{J_1J_2[(z-Z_1)(z-Z_2)(z-Z_3)(z-Z_4)]}.\end{aligned} \tag{B3}$$

Four poles of the function are $Z_{1,2}=\frac{-1\pm\sqrt{1-4J_1J_2}}{2J_1}$ and $Z_{3,4}=\frac{-1\pm\sqrt{1-4J_1J_2}}{2J_2}$ respectively.

It can be shown that $Z_{3,4} = 1/Z_{1,2}$. By Cauchy's residue theorem, the winding number and the phase boundary can be determined. There are three different situations:

$$A: \text{ If } |Z_1| < 1 \text{ and } |Z_2| < 1, \quad \Longrightarrow \quad W = 1, \tag{B4}$$

$$B: \text{ If } |Z_3| < 1 \text{ and } |Z_4| < 1, \quad \Longrightarrow \quad W = -1, \tag{B5}$$

$$C: \text{ If } |Z_1| < 1 \text{ and } |Z_3| < 1, \text{ or } |Z_2| < 1 \text{ and } |Z_4| < 1, \quad \Longrightarrow \quad W = 0. \tag{B6}$$

They are three different gapped phases, where conditions A and B correspond to two different nontrivial topological phases. The corresponding Q matrix elements wind around the origin of the complex plane counterclockwise and clockwise respectively. Phase boundaries are determined by $|Z_{1,2}| = |Z_{3,4}| = 1$, and hence $\mu^*_{\mathbf{k}_\parallel} = \pm 2t_z$, which is consistent with the condition for gap closing. Therefore, we can solve the topological nontrivial conditions for A and B situations, and obtain

$$|\mu^*_{\mathbf{k}_\parallel}| = |-\mu^* + \frac{k^2_{\mathbf{k}_\parallel}}{2m^*}| < 2t^*_z. \tag{B7}$$

[1] E. Majorana, Nuovo Cimento **14**, 171 (2008).
[2] C.-K. Chiu, J. C. Y. Teo, A. P. Schnyder, and S. Ryu, Rev. Mod. Phys. **88**, 035005 (2016).
[3] M. Cheng, M. Zaletel, M. Barkeshli, A. Vishwanath, and P. Bonderson, Phys. Rev. X **6**, 041068 (2016).
[4] A. Y. Kitaev, Phys. Usp. **44**, 131 (2001).
[5] L. Fu and C. L. Kane, Phys. Rev. Lett. **100**, 096407 (2008).
[6] J. D. Sau, R. M. Lutchyn, S. Tewari, and S. Das Sarma, Phys. Rev. Lett. **104**, 040502 (2010).
[7] J. Alicea, Phys. Rev. B **81**, 125318 (2010).
[8] M. Sato, Y. Takahashi, and S. Fujimoto, Phys. Rev. B **82**, 134521 (2010).
[9] R. M. Lutchyn, J. D. Sau, and S. Das Sarma, Phys. Rev. Lett. **105**, 077001 (2010).
[10] V. Mourik, K. Zuo, S. M. Frolov, S. R. Plissard, E. P. A. M. Bakkers, and L. P. Kouwenhoven, Science **336**, 1003 (2012).
[11] A. Das, Y. Ronen, Y. Most, Y. Oreg, M. Heiblum, and H. Shtrikman, Nat. Phys. **8**, 887 (2012).
[12] L. P. Rokhinson, X. Liu, and J. K. Furdyna, Nat. Phys. **8**, 795 (2012).
[13] M. T. Deng, C. L. Yu, G. Y. Huang, M. Larsson, P. Caroff, and H. Q. Xu, Nano Lett. **12**, 6414 (2012).
[14] Q. L. He, L. Pan, A. L. Stern, E. C. Burks, X. Che, G. Yin, J. Wang, B. Lian, Q. Zhou, E. S. Choi, K. Murata, X. Kou, Z. Chen, T. Nie, Q. Shao, Y. Fan, S.-C. Zhang, K. Liu, J. Xia, and K. L. Wang, Science **357**, 294 (2017).
[15] S. Tewari, S. Das Sarma, C. Nayak, C. Zhang, and P. Zoller, Phys. Rev. Lett. **98**, 010506 (2007).
[16] Z. Shermadini, A. Krzton-Maziopa, M. Bendele, R. Khasanov, H. Luetkens, K. Conder, E. Pomjakushina, S. Weyeneth, V. Pomjakushin, O. Bossen, and A. Amato, Phys. Rev. Lett. **106**, 117602 (2011).
[17] X.-J. Liu, K. T. Law, and T. K. Ng, Phys. Rev. Lett. **112**, 086401 (2014).
[18] M. Sato, Y. Takahashi, and S. Fujimoto, Phys. Rev. Lett. **103**, 020401 (2009).
[19] A. K. Fedorov, S. I. Matveenko, V. I. Yudson, and G. V. Shlyapnikov, Sci. Rep. **6** 27448 (2016).
[20] R. Wakatsuki, M. Ezawa, and N. Nagaosa, Phys. Rev. B **89**, 174514 (2014).
[21] R. Wakatsuki, M. Ezawa, Y. Tanaka, and N. Nagaosa, Phys. Rev. B **90**, 014505 (2014).
[22] A. Alecce and L. Dell'Anna, Phys. Rev. B **95**, 195160 (2017).
[23] D. Vodola, L. Lepori, E. Ercolessi, A. V. Gorshkov, and G. Pupillo, Phys. Rev. Lett. **113**, 156402 (2014).
[24] K.-K. Ni, S. Ospelkaus, M. H. G. de Miranda, A. Pe'er, B. Neyenhuis, J. J. Zirbel, S. Kotochigova, P. S. Julienne, D. S. Jin, and J. Ye, Science **322**, 231 (2008).
[25] O.-P. Saira, Y. Yoon, T. Tanttu, M. Möttönen, D. V. Averin, and J. P. Pekola, Phys. Rev. Lett. **109**, 180601 (2012).
[26] J. W. Park, S. A. Will, and M. W. Zwierlein, Phys. Rev. Lett. **114**, 205302 (2015).
[27] M.-S. Heo, T. T. Wang, C. A. Christensen, T. M. Rvachov, D. A. Cotta, J.-H. Choi, Y.-R. Lee, and W. Ketterle, Phys. Rev. A **86**, 021602(R) (2012).
[28] J. Deiglmayr, A. Grochola, M. Repp, K. Mörtlbauer, C. Glück, J. Lange, O. Dulieu, R. Wester, and M. Weidemüller, Phys. Rev. Lett. **101**, 133004 (2008).
[29] M. Repp, R. Pires, J. Ulmanis, R. Heck, E. D. Kuhnle, M. Weidemüller, and E. Tiemann, Phys. Rev. A **87**, 010701(R) (2013).
[30] B. Naylor, A. Reigue, E. Maréchal, O. Gorceix, B. Laburthe-Tolra, and L. Vernac, Phys. Rev. A **91**, 011603(R) (2015).
[31] M. Lu, N. Q. Burdick, and B. L. Lev, Phys. Rev. Lett. **108**, 215301 (2012).
[32] K. Aikawa, A. Frisch, M. Mark, S. Baier, R. Grimm, and F. Ferlaino, Phys. Rev. Lett. **112**, 010404 (2014).
[33] G. Quéméner and J. L. Bohn, Phys. Rev. A **81**, 060701(R) (2010).
[34] A. Micheli, Z. Idziaszek, G. Pupillo, M. A. Baranov, P. Zoller, and P. S. Julienne, Phys. Rev. Lett. **105**, 073202 (2010).
[35] M. H. G. de Miranda, A. Chotia, B. Neyenhuis, D. Wang, G. Quéméner, S. Ospelkaus, J. L. Bohn, J. Ye, and D. S. Jin, Nat. Phys. **7**, 502 (2011).
[36] G. M. Bruun and E. Taylor, Phys. Rev. Lett. **101**, 245301 (2008).
[37] N. R. Cooper and G. V. Shlyapnikov, Phys. Rev. Lett. **103**, 155302 (2009).
[38] J. Levinsen, N. R. Cooper, and G. V. Shlyapnikov, Phys. Rev. A **84**, 013603 (2011).
[39] A. Pikovski, M. Klawunn, G. V. Shlyapnikov, and L. Santos, Phys. Rev. Lett. **105**, 215302 (2010).
[40] K. Sun, C. Wu, and S. Das Sarma, Phys. Rev. B **82**, 075105 (2010).
[41] Y. Yamaguchi, T. Sogo, T. Ito, and T. Miyakawa, Phys. Rev. A **82**, 013643 (2010).
[42] C.-K. Chan, C. Wu, W.-C. Lee, and S. Das Sarma, Phys. Rev. A **81**, 023602 (2010).
[43] L. M. Sieberer and M. A. Baranov, Phys. Rev. A **84**, 063633 (2011).

[44] N. T. Zinner, B. Wunsch, D. Pekker, and D.-W. Wang, Phys. Rev. A **85**, 013603 (2012).
[45] M. M. Parish and F. M. Marchetti, Phys. Rev. Lett. **108**, 145304 (2012).
[46] M. Babadi and E. Demler, Phys. Rev. B **84**, 235124 (2011).
[47] Z.-K. Lu and G. V. Shlyapnikov, Phys. Rev. A **85**, 023614 (2012).
[48] Z.-K. Lu, S. I. Matveenko, and G. V. Shlyapnikov, Phys. Rev. A **88**, 033625 (2013).
[49] N. Matveeva and S. Giorgini, Phys. Rev. Lett. **109**, 200401 (2012).
[50] M. A. Baranov, A. Micheli, S. Ronen, and P. Zoller, Phys. Rev. A **83**, 043602 (2011).
[51] F. Cinti, D.-W. Wang, and M. Boninsegni, Phys. Rev. A **95**, 023622 (2017).
[52] A. C. Potter, E. Berg, D.-W. Wang, B. I. Halperin, and E. Demler, Phys. Rev. Lett. **105**, 220406 (2010).
[53] R. M. Lutchyn, E. Rossi, and S. Das Sarma, Phys. Rev. A **82**, 061604(R) (2010).
[54] S. Ospelkaus, K.-K. Ni, G. Quéméner, B. Neyenhuis, D. Wang, M. H. G. de Miranda, J. L. Bohn, J. Ye, and D. S. Jin, Phys. Rev. Lett. **104**, 030402 (2010).
[55] A. Kitaev and J. Preskill, Phys. Rev. Lett. **96**, 110404 (2006).
[56] M. Levin and X.-G. Wen, Phys. Rev. Lett. **96**, 110405 (2006).
[57] H. Li and F. D. M. Haldane, Phys. Rev. Lett. **101**, 010504 (2008).
[58] F. Pollmann, A. M. Turner, E. Berg, and M. Oshikawa, Phys. Rev. B **81**, 064439 (2010).
[59] A. M. Turner, F. Pollmann, and E. Berg, Phys. Rev. B **83**, 075102 (2011).
[60] S. Ryu and Y. Hatsugai, Phys. Rev. B **73**, 245115 (2006).
[61] M.-C. Chung, Y.-H. Jhu, P. Chen, and S. Yip, Europhys. Lett. **95**, 27003 (2011).
[62] M.-C. Chung, Y.-H. Jhu, P. Chen, and C.-Y. Mou, J. Phys.: Condens. Matter **25**, 285601 (2013).
[63] J.-S. You and D.-W. Wang, New J. Phys. **16**, 073041 (2014).
[64] C. J. Pethick and H. Smith, *Bose-Einstein Condensation in Dilute Gases*, 2nd ed. (Cambridge University Press, Cambridge, UK, 2008).
[65] L. Fidkowski and A. Kitaev, Phys. Rev. B **83**, 075103 (2011).
[66] L. Fidkowski and A. Kitaev, Phys. Rev. B **81**, 134509 (2010).
[67] C. V. Kraus, S. Diehl, P. Zoller, and M. A. Baranov, New J. Phys. **14**, 113036 (2012).